Eur. Phys. J. A **31**, 875–882 (2007)
DOI 10.1140/epja/i2006-10284-4

THE EUROPEAN PHYSICAL JOURNAL A

Special Article – QNP 2006

Scenario of instabilities driven equilibration of the quark-gluon plasma

St. Mrówczyński[a]

Institute of Physics, Świętokrzyska Academy, ul. Świętokrzyska 15, PL - 25-406 Kielce, Poland and
Sołtan Institute for Nuclear Studies, ul. Hoża 69, PL - 00-681 Warsaw, Poland

Received: 18 December 2006
Published online: 20 March 2007 –

Abstract. Due to anisotropic momentum distribution the parton system produced at the early stage of relativistic heavy-ion collisions is unstable with respect to the magnetic plasma modes. The instabilities isotropize the system and thus speed up the process of its equilibration. The scenario of instabilities-driven isotropization is reviewed.

PACS. 12.38.Mh Quark-gluon plasma – 25.75.-q Relativistic heavy-ion collisions

1 Introduction

The matter created in relativistic heavy-ion collisions manifests a strongly collective hydrodynamic behaviour [1] which is particularly evident in studies of the so-called elliptic flow [2]. Hydrodynamic description requires, strictly speaking, a local thermal equilibrium and experimental data on the particle spectra and elliptic flow suggest, when analysed within the hydrodynamic model, that an equilibration time of the parton[1] system is as short as $0.6\,\mathrm{fm}/c$ [1]. Such a fast equilibration can be explained assuming that the quark-gluon plasma (QGP) is strongly coupled [3]. However, it is far not excluded that due to the high-energy density at the early stage of the collision, when the elliptic flow is generated, the plasma is weakly coupled because of the asymptotic freedom. Thus, the question arises whether the weakly interacting plasma can be equilibrated within $1\,\mathrm{fm}/c$.

Calculations, which assume that the parton-parton collisions are responsible for the equilibration of the weakly interacting QGP, provide an equilibration time of at least $2.6\,\mathrm{fm}/c$ [4]. To thermalize the system one needs either a few hard collisions of the momentum transfer of order of the characteristic parton momentum[2], which is denoted here as T (as the temperature of equilibrium system), or many collisions of smaller transfer. As discussed in *e.g.* [5], the inverse time scale of the collisional equilibration is of order $g^4 \ln(1/g)\, T$, where g is the QCD coupling constant. However, the equilibration is speeded up by instabilities generated in an anisotropic QGP [6–8], as growth of the unstable modes is associated with the system's isotropization. The characteristic inverse time of instability development is roughly of order gT for a sufficiently anisotropic momentum distribution [6,9–11]. Thus, the instabilities are much "faster" than the collisions in the weak-coupling regime. Recent numerical simulation [12] shows that the instabilities-driven isotropization is indeed very efficient.

The isotropization should be clearly distinguished from the equilibration. The instabilities-driven isotropization is a mean-field reversible phenomenon which is *not* accompanied with the entropy production [6,12]. Therefore, the collisions, which are responsible for the dissipation, are needed to reach the equilibrium state of maximal entropy. The instabilities contribute to the equilibration indirectly, shaping the parton momenta distribution.

A large variety of instabilities of the electron-ion plasma are known [13]. Those caused by coordinate space inhomogeneities, in particular by the system's boundaries, are usually called *hydrodynamic* instabilities while those due to non-equilibrium momentum distribution of plasma particles are called *kinetic* instabilities. Hardly anything is known about QGP hydrodynamic instabilities, and I will not speculate about them. The kinetic instabilities are initiated either by the charge or current fluctuations. In the first case, the electric field ($\mathbf{E}$) is longitudinal ($\mathbf{E} \parallel \mathbf{k}$, where $\mathbf{k}$ is the wave vector), while in the second case the field is transverse ($\mathbf{E} \perp \mathbf{k}$). For this reason, the kinetic instabilities caused by the charge fluctuations are usually called *longitudinal* while those caused by the current fluctuations are called *transverse*. Since the electric field plays a crucial role in the longitudinal mode generation, the

[a] e-mail: mrow@fuw.edu.pl

[1] The term "parton" is used to denote quark or gluon.

[2] Although an anisotropic system is considered, the characteristic momentum in all directions is assumed to be of the same order.

longitudinal instabilities are also called *electric* while the transverse ones are called *magnetic*. The electric instabilities, which occur in systems with multi-bump momentum distributions [13], are rather irrelevant for QGP produced in relativistic heavy-ion collisions. For this reason the longitudinal modes are not discussed here. The magnetic mode known as the filamentation or Weibel instability appears to be relevant because a momentum anisotropy is a sufficient condition for its existence. In the following sections a whole scenario of the instabilities-driven isotropization is discussed. A more extensive account of the scenario is given in [14] where, in particular, other approaches to the problem of QGP thermalization are also presented. Here, however, very recent developments are briefly discussed.

2 Seeds of the filamentation and its mechanism

Let me consider a non-equilibrium parton system which is homogeneous but the parton momentum distribution is anisotropic. The system is on average locally colourless but colour fluctuations are possible. Therefore, $\langle j_a^\mu(x)\rangle = 0$, where $j_a^\mu(x)$ is a local colour four-current in the adjoint representation of $SU(N_c)$ gauge group with $\mu = 0,1,2,3$ and $a = 1,2,\ldots,N_c^2-1$ being the Lorentz and colour index, respectively; $x = (t,\mathbf{x})$ denotes a four-position in the coordinate space. As discussed in [15], the current correlator for a classical system of free partons is

$$M_{ab}^{\mu\nu}(t,\mathbf{x}) \stackrel{\text{def}}{=} \langle j_a^\mu(t_1,\mathbf{x}_1) j_b^\nu(t_2,\mathbf{x}_2)\rangle = \frac{1}{8} g^2 \delta^{ab} \int \frac{\mathrm{d}^3p}{(2\pi)^3}\, \frac{p^\mu p^\nu}{E_p^2}\, f(\mathbf{p})\, \delta^{(3)}(\mathbf{x}-\mathbf{v}t), \quad (1)$$

where $(t,\mathbf{x}) \equiv (t_2-t_1, \mathbf{x}_2-\mathbf{x}_1)$, $\mathbf{v} \equiv \mathbf{p}/E_p$ and the effective parton distribution function $f(\mathbf{p})$ equals $n(\mathbf{p}) + \bar{n}(\mathbf{p}) + 2N_c n_g(\mathbf{p})$ with $n(\mathbf{p})$, $\bar{n}(\mathbf{p})$ and $n_g(\mathbf{p})$ giving the average colourless distribution function of quarks $Q^{ij}(x,\mathbf{p}) = \delta^{ij} n(\mathbf{p})$, of antiquarks $\bar{Q}^{ij}(x,\mathbf{p}) = \delta^{ij}\bar{n}(\mathbf{p})$, and of gluons $G^{ab}(x,\mathbf{p}) = \delta^{ab} n_g(\mathbf{p})$. We note that the distribution function of (anti)quarks belongs to the fundamental representation of the $SU(N_c)$ group while that of gluons to the adjoint representation. Therefore, $i,j = 1,2,\ldots,N_c$ and $a,b = 1,2,\ldots,N_c^2-1$.

Due to the average space-time homogeneity, the correlation tensor (1) depends only on the difference $(t_2 - t_1, \mathbf{x}_2 - \mathbf{x}_1)$. The space-time points $(t_1,\mathbf{x}_1)$ and $(t_2,\mathbf{x}_2)$ are correlated in the system of non-interacting particles if a particle travels from $(t_1,\mathbf{x}_1)$ to $(t_2,\mathbf{x}_2)$. For this reason the delta $\delta^{(3)}(\mathbf{x}-\mathbf{v}t)$ is present in the formula (1). The momentum integral of the distribution function simply represents the sum over particles. The fluctuation spectrum is found as a Fourier transform of the tensor (1),

$$M_{ab}^{\mu\nu}(\omega,\mathbf{k}) = \frac{1}{8} g^2\, \delta^{ab} \int \frac{\mathrm{d}^3p}{(2\pi)^3}\, \frac{p^\mu p^\nu}{E_p^2}\, f(\mathbf{p})\, 2\pi\delta(\omega - \mathbf{k}\mathbf{v}). \quad (2)$$

To compute the fluctuation spectrum, the parton momentum distribution has to be specified. Such calculations with two forms of the anisotropic momentum distribution are presented in [15]. Here I only qualitatively discuss eqs. (1), (2). I assume that the momentum distribution is elongated in, say, the z-direction. Then, eqs. (1), (2) clearly show that the correlator M^{zz} is larger than M^{xx} or M^{yy}. It is also clear that M^{zz} is the largest when the wave vector $\mathbf{k}$ is along the direction of the momentum deficit. Then, the delta function $\delta(\omega - \mathbf{k}\mathbf{v})$ does not much constrain the integral in eq. (2). Since the momentum distribution is elongated in the z-direction, the current fluctuations are the largest when the wave vector $\mathbf{k}$ is the xy-plane. Thus, I conclude that some fluctuations in the anisotropic system are large, much larger than in the isotropic one. An anisotropic system has a natural tendency to split into the current filaments parallel to the direction of the momentum surplus. These currents are seeds of the filamentation instability.

Let me now explain in terms of elementary physics why the fluctuating currents, which flow in the direction of the momentum surplus, can grow in time. To simplify the discussion, which follows [15], I consider an electromagnetic anisotropic system. The form of the fluctuating current is chosen to be

$$\mathbf{j}(x) = j\, \hat{\mathbf{e}}_z\, \cos(k_x x), \quad (3)$$

where $\hat{\mathbf{e}}_z$ is the unit vector in the z-direction. We have the current filaments of thickness $\pi/|k_x|$ with the current flowing in the opposite directions in the neighbouring filaments. The magnetic field $\mathbf{B}$ generated by the current (3) is oriented along the axis y and the Lorentz force acting on the partons, which fly in the z-direction, is

$$\mathbf{F}(x) = q\,\mathbf{v}\times\mathbf{B}(x) = -q\, v_z\, \frac{j}{k_x}\, \hat{\mathbf{e}}_x\, \sin(k_x x),$$

where q is the electric charge. One observes, see fig. 1, that the force distributes the partons in such a way that those, which positively contribute to the current in a given filament, are focused in the filament centre while those, which negatively contribute, are moved to the neighbouring one. Thus, the initial current grows. For a somewhat different explanation see [11].

3 Dispersion equation

The equation of motion of the Fourier-transformed chromodynamic field $A^\mu(k)$ is

$$\Big[k^2 g^{\mu\nu} - k^\mu k^\nu - \Pi^{\mu\nu}(k)\Big] A_\nu(k) = 0, \quad (4)$$

where $\Pi^{\mu\nu}(k)$ is the polarization tensor or gluon self-energy which is discussed later on. A general plasmon dispersion equation is of the form

$$\det\Big[k^2 g^{\mu\nu} - k^\mu k^\nu - \Pi^{\mu\nu}(k)\Big] = 0. \quad (5)$$

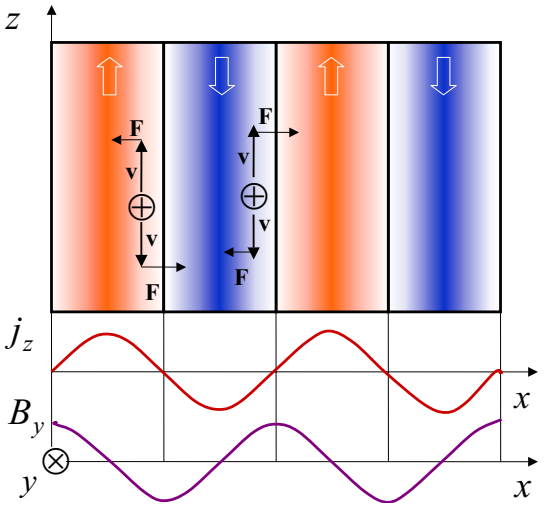

Fig. 1. The mechanism of filamentation instability, see text for the description.

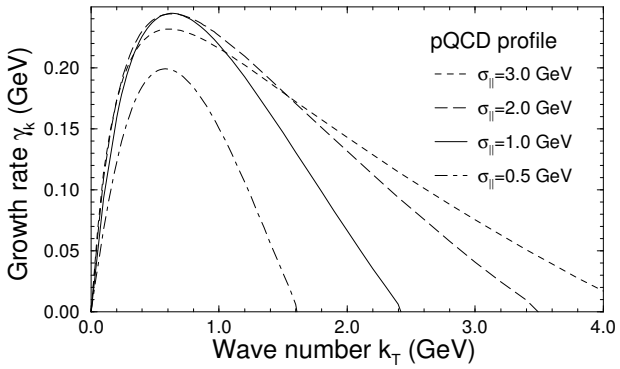

Fig. 2. The growth rate of the unstable mode as a function of the wave vector $\mathbf{k} = (k_\perp, 0, 0)$ for $\sigma_\perp = 0.3\,\mathrm{GeV}$ and 4 values of the parameter $\sigma_\parallel$ which controls the system's anisotropy. The figure is taken from [9].

The polarization tensor, which can be derived in the linear response approximation either within the transport theory or diagrammatically [16], is

$$\Pi^{\mu\nu}(k) = \frac{g^2}{2}\int \frac{\mathrm{d}^3p}{(2\pi)^3}\frac{f(\mathbf{p})}{|\mathbf{p}|}\left[\frac{(p\cdot k)(k^\mu p^\nu + p^\mu k^\nu)}{(p\cdot k)^2} - \frac{k^2 p^\mu p^\nu + (p\cdot k)^2 g^{\mu\nu}}{(p\cdot k)^2}\right], \tag{6}$$

where $f(\mathbf{p})$ is the already defined effective parton distribution function; the spin and flavour are treated as parton internal degrees of freedom. The quarks and gluons are assumed to be massless. Since $\Pi^{\mu\nu}(k)$ is the unit matrix in the colour space, the colour indices are suppressed.

Due to the transversality of $\Pi^{\mu\nu}(k)$ ($k_\mu\Pi^{\mu\nu}(k) = k_\nu\Pi^{\mu\nu}(k) = 0$) not all components of $\Pi^{\mu\nu}(k)$ are independent of each other, and consequently the dispersion equation (5), which involves a determinant of 4×4 matrix, can be simplified to the determinant of 3×3 matrix. For this purpose, I introduce the chromoelectric permittivity tensor $\epsilon^{lm}(k)$, where the indices $l, m, n = 1, 2, 3$ label three-vector and tensor components. Because $\epsilon^{lm}(k)E^l(k)E^m(k) = \Pi^{\mu\nu}(k)A_\mu(k)A_\nu(k)$, where $\mathbf{E}$ is the chromoelectric vector, the permittivity can be expressed through the polarization tensor as $\epsilon^{lm}(k) = \delta^{lm} + \Pi^{lm}(k)/\omega^2$. Then, the dispersion equation gets the form

$$\det\left[\mathbf{k}^2\delta^{lm} - k^l k^m - \omega^2\epsilon^{lm}(k)\right] = 0. \tag{7}$$

Substituting the permittivity $\epsilon^{lm}(k)$ into eq. (7), one fully specifies the dispersion equation (7) which provides a spectrum of quasi-particle bosonic excitations. A solution $\omega(\mathbf{k})$ of eq. (7) is called *stable* when $\mathrm{Im}\,\omega \le 0$ and it is called *unstable* when $\mathrm{Im}\,\omega > 0$. In the first case the amplitude is constant or it exponentially decreases in time while in the second one there is an exponential growth of the amplitude. In practice, it appears difficult to find solutions of eq. (7) because of the rather complicated structure of the dielectric tensor. A quite general analysis of the dispersion equation of the anisotropic system is given in [10]. The problem simplifies as we are interested in specific modes which are expected to be unstable. Namely, we look for solutions corresponding to the fluctuating current in the direction of the momentum surplus and the wave vector perpendicular to it.

As previously, the momentum distribution is assumed to be elongated in the z-direction, and consequently the fluctuating current also flows in this direction. The magnetic field has a non-vanishing component along the y-direction and the electric filed is in the z-direction. Finally, the wave vector is parallel to the axis x, see fig. 1. It is also assumed that the momentum distribution obeys the mirror symmetry $f(-\mathbf{p}) = f(\mathbf{p})$, and then the permittivity tensor has only non-vanishing diagonal components. Taking into account all these conditions, one simplifies the dispersion equation (7) to the form

$$H(\omega) \equiv k_x^2 - \omega^2\epsilon^{zz}(\omega, k_x) = 0. \tag{8}$$

The existence of unstable solutions of eq. (8) can be proved without solving it. The so-called Penrose criterion [13], which follows from analytic properties of the permittivity as a function of ω, states that *the dispersion equation $H(\omega) = 0$ has unstable solutions if $H(\omega = 0) < 0$*. The Penrose criterion was applied to eq. (8) in [6]. A more general discussion of the instability condition is presented in [11]. Without entering into details, there exist unstable modes if the momentum distribution averaged (with a proper weight) over momentum length is anisotropic.

To solve the dispersion equation (8), the parton momentum distribution has to be specified. Several analytic (usually approximate) solutions of the dispersion equation can be found in [6,10,11]. A typical example of the numerical solution, which gives the unstable mode frequency in the full range of wave vectors is shown in fig. 2 taken from [9]. The mode is pure imaginary and $\gamma_k \equiv \mathrm{Im}\,\omega(k_\perp)$. The parameters $\sigma_\parallel$ and $\sigma_\perp$ control the widths of longitudinal (z) and transverse momentum distributions; the coupling is $\alpha_s \equiv g^2/4\pi = 0.3$, and the effective parton density

is chosen to be $6\,\mathrm{fm}^{-3}$. As seen, there is a finite interval of wave vectors for which the unstable modes exist.

4 Isotropization and Abelianization

When the instabilities grow the system becomes more isotropic because the Lorentz force changes particle's momenta and the growing fields carry an extra momentum. To explain the mechanism I assume, as previously, that initially there is a momentum surplus in the z-direction. The fluctuating current tends to flow in the z-direction with the wave vector pointing in the x-direction. Since the magnetic field has a y component, the Lorentz force, which acts on partons flying along the z-axis, pushes the partons in the x-direction where there is a momentum deficit. Numerical simulations discussed in the next section show the efficiency of the mechanism.

The system isotropizes not only due to the effect of the Lorentz force but also due to the momentum carried by the growing field. When the magnetic and electric fields are oriented along the y and z axes, respectively, the Poynting vector points in the direction x that is along the wave vector. Thus, the momentum carried by the fields is oriented in the direction of the momentum deficit of particles.

One wonders whether non-Abelian non-linearities do not stabilize the unstable modes. An elegant argument [17] suggests that this is not the case as the system spontaneously chooses an Abelian configuration in the course of instability development. Let me explain the idea.

In the Coulomb gauge the effective potential of the unstable configuration has the form

$$V_{\mathrm{eff}}[\mathbf{A}^a] = -\mu^2 \mathbf{A}^a \cdot \mathbf{A}^a + \frac{1}{4} g^2 f^{abc} f^{ade} (\mathbf{A}^b \mathbf{A}^d)(\mathbf{A}^c \mathbf{A}^e),$$

which is shown in fig. 3 taken from [17]. The first term (with $\mu^2 > 0$) is responsible for the very existence of the instability. The second term, which comes from the Yang-Mills Lagrangian, is of pure non-Abelian nature. The term is positive and thus it counteracts the instability growth. However, the non-Abelian term vanishes when the potential $\mathbf{A}^a$ is effectively Abelian, and consequently, such a configuration corresponds to the steepest decrease of the effective potential. Thus, the system spontaneously abelianizes in the course of instability growth. The abelianization is further discussed in sect. 7.

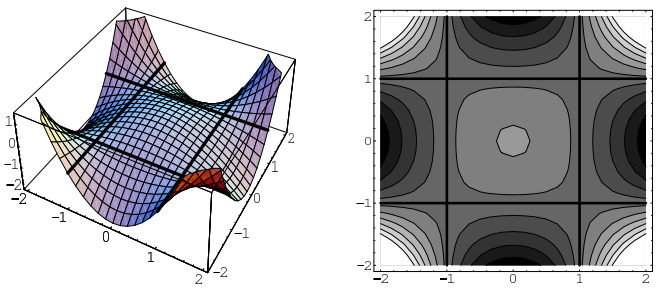

Fig. 3. The effective potential of the unstable magnetic mode as a function of magnitude of two colour components of $\mathbf{A}^a$ belonging to the $SU(2)$ gauge group. The figure is taken from [17].

5 Hard-loop effective action

Knowledge of the gluon polarization tensor or, equivalently, the chromoelectric permittivity tensor is sufficient to discuss the system's stability and the dispersion relations of unstable modes. For more detailed dynamical studies the effective action of anisotropic QGP is needed. Such an action for a system, which is on average locally colour neutral, stationary and homogeneous, was derived in [18], see also [19]. The starting point was the effective action which describes an interaction of classical fields with currents induced by these fields in the plasma. The Lagrangian density is quadratic in the gluon and quark fields and it equals

$$\mathcal{L}_2(x) = -\int \mathrm{d}^4 y \left(\frac{1}{2} A^a_\mu(x) \Pi^{\mu\nu}_{ab}(x-y) A^b_\nu(y) + \bar{\Psi}(x) \Sigma(x-y) \Psi(y) \right); \tag{9}$$

the Fourier-transformed gluon polarization tensor $\Pi^{\mu\nu}_{ab}(k)$ is given by eq. (6) while the quark self-energy $\Sigma(k)$ reads [16,20]

$$\Sigma(k) = g^2 \frac{N_c^2 - 1}{8 N_c} \int \frac{\mathrm{d}^3 p}{(2\pi)^3} \frac{\tilde{f}(\mathbf{p})}{|\mathbf{p}|} \frac{p \cdot \gamma}{p \cdot k}, \tag{10}$$

where $\tilde{f}(\mathbf{p}) \equiv n(\mathbf{p}) + \bar{n}(\mathbf{p}) + 2 n_g(\mathbf{p})$. The action (9) holds under the assumption that the field amplitude is much smaller than T/g, where T denotes the characteristic momentum of (hard) partons.

Following Braaten and Pisarski [21], the Lagrangian (9) was modified to comply with the requirement of gauge invariance. The final result, which is non-local but manifestly gauge invariant, is [18]

$$\mathcal{L}_{\mathrm{HL}}(x) = \frac{g^2}{2} \int \frac{\mathrm{d}^3 p}{(2\pi)^3} \left[f(\mathbf{p})\, F^a_{\mu\nu}(x) \left(\frac{p^\nu p^\rho}{(p \cdot D)^2} \right)_{ab} F_\rho{}^{b\,\mu}(x) + i \frac{N_c^2 - 1}{4 N_c} \tilde{f}(\mathbf{p})\, \bar{\Psi}(x) \frac{p \cdot \gamma}{p \cdot D} \Psi(x) \right], \tag{11}$$

where $F^{\mu\nu}_a$ is the strength tensor and D denotes the covariant derivative. The effective action (11) generates n-point functions which obey the Ward-Takahashi identities. For the equilibrium plasma the action (11) is equivalent to that derived in [22] and in the explicitly gauge-invariant form in [21]. The equilibrium hard-loop action was also found within the semiclassical kinetic theory [23,24].

6 Equations of motion

Transport theory provides a natural framework to study temporal evolution of non-equilibrium systems and it has been applied to QGP for a long time. The distribution functions of quarks (Q), antiquarks ($\bar{Q}$), and gluons (G),

which are the $N_c \times N_c$ and $(N_c^2-1)\times(N_c^2-1)$ matrices, respectively, satisfy the transport equations of the form [25,26]:

$$p^\mu D_\mu Q(\mathbf{p},x) + \frac{g}{2}\, p^\mu \left\{ F_{\mu\nu}(x), \frac{\partial Q(\mathbf{p},x)}{\partial p_\nu} \right\} = 0,$$

$$p^\mu D_\mu \bar{Q}(\mathbf{p},x) - \frac{g}{2}\, p^\mu \left\{ F_{\mu\nu}(x), \frac{\partial \bar{Q}(\mathbf{p},x)}{\partial p_\nu} \right\} = 0, \qquad (12)$$

$$p^\mu \mathcal{D}_\mu G(\mathbf{p},x) + \frac{g}{2}\, p^\mu \left\{ \mathcal{F}_{\mu\nu}(x), \frac{\partial G(\mathbf{p},x)}{\partial p_\nu} \right\} = 0,$$

where $\{\ldots,\ldots\}$ denotes the anticommutator; the transport equation of (anti)quarks is written down in the fundamental representation while that of gluons in the adjoint one. Since the instabilities of interest are very fast, much faster than the inter-parton collisions, the collision terms are neglected in eqs. (12). The gauge field, which enters the transport equations (12), is generated self-consistently by the quarks and gluons. Thus, the transport equations (12) should be supplemented by the Yang-Mills equation

$$D_\mu F^{\mu\nu}(x) = j^\nu(x), \qquad (13)$$

where the colour current is given as

$$j^\mu(x) = -g \int \frac{\mathrm{d}^3 p}{(2\pi)^3}\, \frac{p^\mu}{|\mathbf{p}|}\, \tau_a \,\mathrm{Tr}\left[\tau_a\left(Q-\bar{Q}\right) + T_a G\right], \qquad (14)$$

with τ_a and T_a being the $SU(N_c)$ group generators in the fundamental and adjoint representation, respectively. There is a version of eqs. (12), (13) where colour charges of partons are treated as a classical variable [27]. Then, the distribution functions depend not only on x and $\mathbf{p}$ but on the colour variable as well.

When eqs. (12), (13) are linearized around the state, which is stationary, homogeneous and locally colourless, the equations provide the hard-loop dynamics encoded in the effective action (11). The equations are of particularly simple and elegant form when the quark $\delta Q(\mathbf{p},x)$, antiquark $\delta\bar{Q}(\mathbf{p},x)$ and gluon $\delta G(\mathbf{p},x)$ deviations from the stationary state described by $Q_0^{ij}(\mathbf{p}) = \delta^{ij} n(\mathbf{p})$, $\bar{Q}_0^{ij}(\mathbf{p}) = \delta^{ij}\bar{n}(\mathbf{p})$, and $G_0^{ab}(\mathbf{p}) = \delta^{ab} n_g(\mathbf{p})$ are parameterised by the field $W^\mu(\mathbf{v},x)$ through the relations

$$\delta Q(\mathbf{p},x) = g\frac{\partial n(\mathbf{p})}{\partial p^\mu} W^\mu(\mathbf{v},x),$$

$$\delta\bar{Q}(\mathbf{p},x) = -g\frac{\partial \bar{n}(\mathbf{p})}{\partial p^\mu} W^\mu(\mathbf{v},x),$$

$$\delta G(\mathbf{p},x) = g\frac{\partial n_g(\mathbf{p})}{\partial p^\mu} T_a \,\mathrm{Tr}\left[\tau_a W^\mu(\mathbf{v},x)\right],$$

where $\mathbf{v} \equiv \mathbf{p}/|\mathbf{p}|$. Then, instead of the three transport equations (12) one has one equation

$$v_\mu D^\mu W^\nu(\mathbf{v},x) = -v_\rho F^{\rho\nu}(x) \qquad (15)$$

while the Yang-Mills equation (13) reads

$$D_\mu F^{\mu\nu}(x) = -g^2 \int \frac{\mathrm{d}^3 p}{(2\pi)^3}\, \frac{p^\nu}{|\mathbf{p}|}\, \frac{\partial f(\mathbf{p})}{\partial p^\rho} W^\rho(\mathbf{v},x), \qquad (16)$$

where $v^\mu = (1,\mathbf{v})$. In contrast to the effective action (11), eqs. (15), (16) are local in coordinate space. Therefore, the transport equation (15) combined with eq. (16) is often called the local representation of the hard-loop dynamics. Equations (15), (16), which for the isotropic equilibrium plasma were first given in [28], are used in the numerical simulations [7,29–32] discussed in the next section.

Recently the fluid equations, which are applicable to short-time scale colour phenomena in QGP, have been derived [33] from the kinetic equations (12). The quantities, which enter the equations, like the hydrodynamic velocity or pressure are gauge dependent matrices in the colour space. The chromo-hydrodynamic approach is designed for numerical studies of the dynamics of the unstable QGP.

7 Numerical simulations

Temporal evolution of the anisotropic QGP was studied by means of numerical simulations [7,12,29–31,34,32, 35]. The dynamics governed by a complete hard-loop action [18], was simulated in [7,29–32]. These simulations provide fully reliable information on the field dynamics but particles are included as a stationary (anisotropic) background. The simulations [12,34,35] treat the quark-gluon system completely classically: partons, which carry classical colour charges, interact with a self-consistently generated classical chromodynamic field. The simulations [7,12] were effectively performed in $1+1$ dimensions as the chromodynamic potentials depend on time and one space variable. The calculations [29,30] represent full $1+3$ dimensional dynamics. In most cases the $SU(2)$ gauge group was studied but some $SU(3)$ results, which are qualitatively very similar to $SU(2)$ ones, are given in [30]. The techniques of discretization used in [7,12,29,30] are rather different while the initial conditions are quite similar. The initial field amplitudes are distributed according to the Gaussian noise and the momentum distribution of partons is strongly anisotropic.

In fig. 4, taken from [7], the results of the hard-loop simulation performed in $1+1$ dimensions are shown. One observes exponential growth of the field energy density which is dominated, as expected, by the magnetic field which is transverse to the direction of the momentum deficit. The growth rate appears to be equal to that of the fastest unstable mode (γ^*). Figure 5, taken from [12], shows results of the classical simulation on the $(1+1)$-dimensional lattice of physical size $L = 40\,\mathrm{fm}$. As in fig. 4, the amount of field energy grows exponentially and the magnetic contribution dominates.

The Abelian ($U(1)$) and non-Abelian ($SU(2)$) results of the $(1+1)$-dimensional simulation presented in fig. 5 are remarkably similar to each other. The abelianization appears to be very efficient in $1+1$ dimensions, as shown in

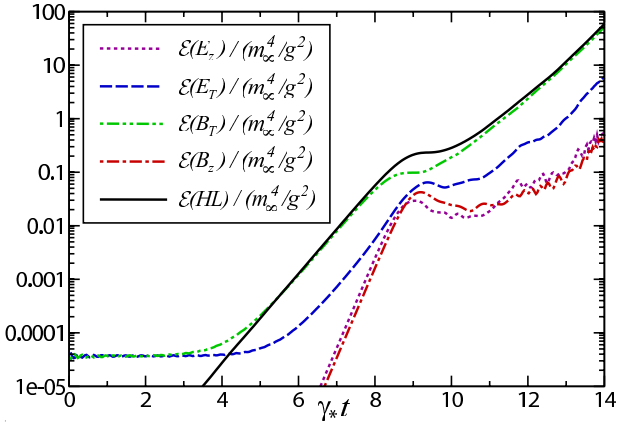

Fig. 4. Time evolution of the (scaled) energy density (split into various electric and magnetic components) which is carried by the chromodynamic field. The simulation is (1+1)-dimensional and the gauge group is $SU(2)$. The parton momentum distribution is squeezed along the z-axis. The solid line corresponds to the total energy transferred from the particles. The figure is taken from [7].

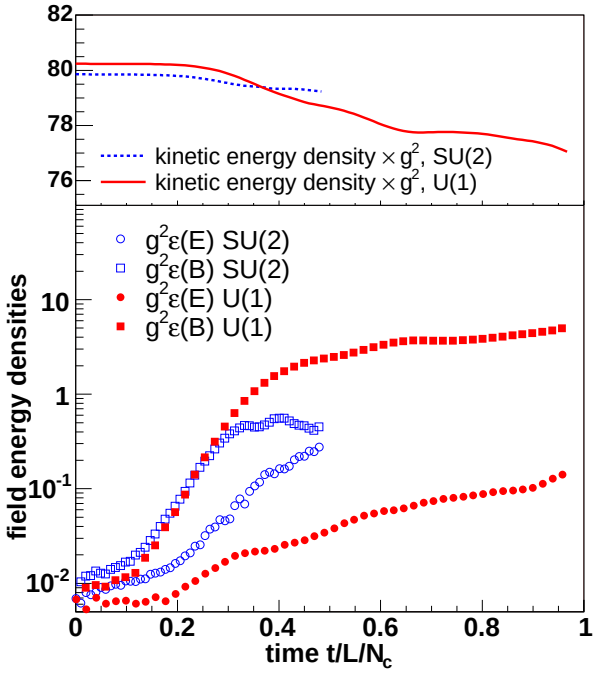

Fig. 5. Time evolution of the kinetic energy of particles (upper panel) and of the energy of electric and magnetic fields (lower panel). The figure is taken from [12].

figs. 6, 7, taken from [12] and [7], respectively. The authors of [12] analysed the functionals:

$$\phi_{\rm rms} \equiv \sqrt{\int_0^L \frac{{\rm d}x}{L}(A_y^a A_y^a + A_z^a A_z^a)}\,,$$
$$\bar{C} \equiv \int_0^L \frac{{\rm d}x}{L}\frac{\sqrt{{\rm Tr}[(i[A_y, A_z])^2]}}{{\rm Tr}[A_y^2 + A_z^2]}\,. \qquad (17)$$

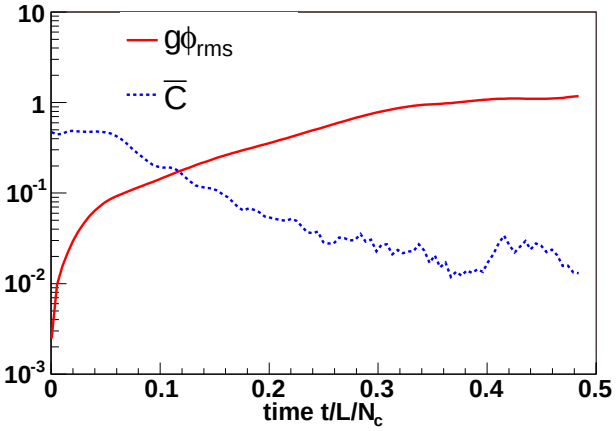

Fig. 6. Temporal evolution of the functionals $\bar{C}$ and $\phi_{\rm rms}$ measured in GeV. The figure is taken from [12].

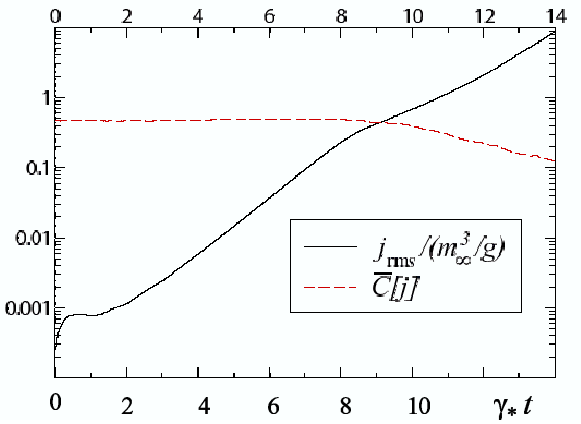

Fig. 7. Temporal evolution of the (scaled) functionals $\bar{C}$ and $j_{\rm rms}$. The figure is taken from [7].

The quantities $j_{\rm rms}$ and $\bar{C}$, studied in [7] and shown in fig. 7, are fully analogous to $\phi_{\rm rms}$ and $\bar{C}$ defined by eq. (17) but the components of the chromodynamic potential are replaced by the respective components of the colour current. As seen in figs. 6, 7, the field (current) commutator decreases in time although the magnitude of the field (current), as quantified by $\phi_{\rm rms}$ ($j_{\rm rms}$), grows.

The results of the $(1+3)$-dimensional simulations [29, 30] are qualitatively different from those of $1+1$ dimensions. As seen in figs. 8, 9, taken from [29,30], respectively, the growth of the field energy density is exponential only for some time, and then the growth becomes approximately linear. The regime changes when the field's amplitude is of order k/g, where k is the characteristic wave vector. Then, the non-Abelian effects start to be important. Figure 10 taken from [29] demonstrates that the abelianization is efficient in $1+3$ dimensions only for a finite interval of time. The commutator C shown in fig. 10 is a natural generalization of the $(1+1)$-dimensional commutator defined by eq. (17).

The regime of linear growth of the magnetic energy, shown in figs. 8, 9 was studied numerically in [31]. It was found that when the exponential growth of the magnetic

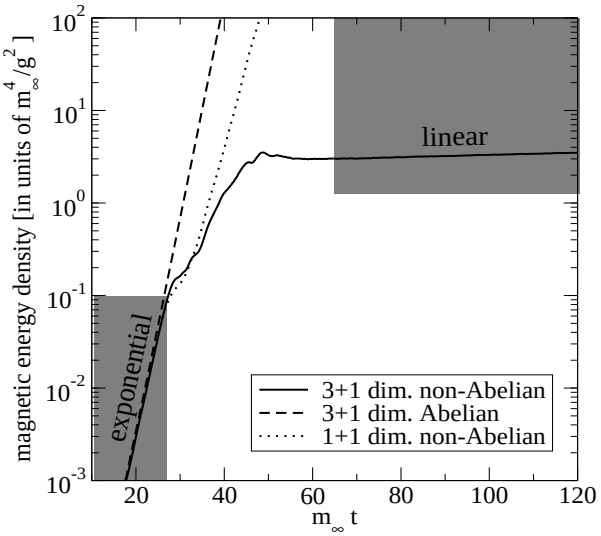

Fig. 8. Time evolution of the (scaled) chromomagnetic energy density in the $(1+3)$-dimensional simulation. The Abelian result and that of $1+1$ dimensions are also shown. The figure is taken from [29].

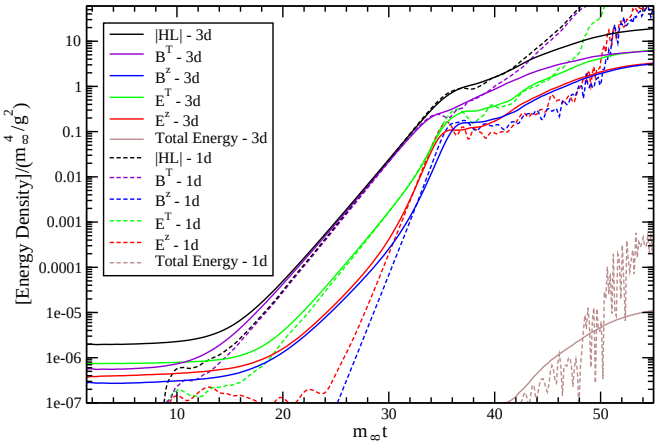

Fig. 9. Time evolution of the (scaled) energy density (split into various electric and magnetic components) of the chromodynamic field in the $1+1$ and $1+3$ simulations. "HL" denotes the total energy contributed by hard particles. The figure is taken from [30].

energy ends, the long-wavelength modes associated with the instability stop growing, but that they cascade energy towards the ultraviolet in the form of plasmon excitations and a quasi-stationary state with the power law distribution k^{-2} of the plasmon mode population appears. The phenomenon was argued [31] to be very similar to the Kolmogorov wave turbulence where the long-wavelength modes transfer their energy without dissipation to the shorter and shorter ones.

A different picture of the non-Abelian regime emerges from the classical simulation [35] where the system with strong momentum anisotropy was studied. When the field strength is high enough, the energy drained by the Weibel-like plasma instability from the particles does not build up exponentially in magnetic fields but instead returns

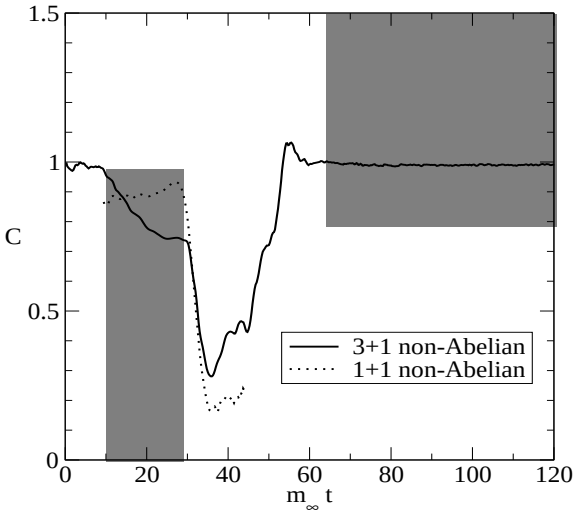

Fig. 10. Temporal evolution of the field commutator quantified by C. The figure is taken from [29].

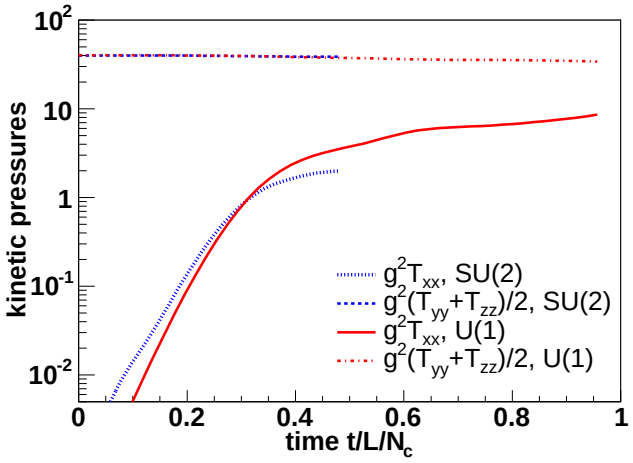

Fig. 11. Temporal evolution of the energy-momentum tensor components T^{xx} and $(T^{yy}+T^{zz})/2$. The Abelian and non-Abelian results are shown. The figure is taken from [12].

isotropically to the ultraviolet not via the quasi-stationary process, as argued in [31], but via a rapid avalanche.

The effect of isotropization of particle momentum distribution due to the action of the Lorentz force is nicely seen in the $(1+1)$-dimensional classical simulation [12]. In fig. 11 taken from [12] there are shown diagonal components of the energy-momentum tensor $T^{\mu\nu}$. The initial momentum distribution is such that $T^{xx}=0$. As seen, T^{xx} exponentially grows.

The numerical studies discussed so far deal with the quark-gluon system of constant volume. A very elegant formulation of the hard-loop dynamics of the system, which experiences the boost invariant expansion in one direction, is given in [32]. In agreement with the earlier expectations [9,11], the expansion is shown both numerically and analytically [32] to slow down the growth of instabilities even when the initial state is highly anisotropic. The field amplitude does not grow exponentially with time

but rather as the exponent of $\sqrt{t}$. The effect of expansion requires further quantitative analysis, as the instabilities might occur irrelevant for heavy-ion collisions, if they are not fast enough to cope with the system's expansion.

An attempt to study an unstable parton system in the conditions close to those, which are realized in relativistic heavy-ion collisions, was undertaken in [36–38]. The system was described in terms of the colour glass condensate approach [39] where small-x partons of large occupation numbers, which dominate the wave functions of incoming nuclei, are treated as classical Yang-Mills fields. Hard modes of the classical fields play the role of particles. The instabilities, identified as the Weibel modes, appear to be generated when the system of Yang-Mills fields expands into the vacuum.

8 Outlook

Although an impressive progress has been achieved, the numerical simulations are still quite far from a real situation met in relativistic heavy-ion collisions. Complete $(1+3)$-dimensional simulations are needed as the results of [29,30] show that the dimensionality crucially matters. The system expansion needs to be incorporated. The effect of back reaction of fields on the particles is fully included only in the classical simulations [12,35–38]. The effect is difficult to study in quantum field approaches as it goes beyond the hard-loop physics which has appeared very rich and complex [29,30]. An attempt to go beyond the hard-loop approximation was undertaken in [40] where the higher-order terms of the effective potential of the anisotropic system were found. Since these terms can be negative, the instability is then driven not only by the negative quadratic term but by the higher-order terms as well.

The coupling constant is assumed to be small in all studies of the unstable parton systems. This is certainly a severe limitation as the phenomenology of heavy-ion collisions suggests that QGP manifests very small viscosity characteristic for strongly coupled systems [3]. However, it has been recently argued [41,42] that an anomalously small viscosity of the quark-gluon system can arise from interactions with turbulent colour fields dynamically generated by the instabilities. Therefore, it might well be that the scenario of instabilities-driven equilibration does not only solve the problem of fast thermalization but other puzzling features of QGP.

References

1. U.W. Heinz, AIP Conf. Proc. **739**, 163 (2005).
2. F. Retiere, J. Phys. G **30**, S827 (2004).
3. E. Shuryak, J. Phys. G **30**, S1221 (2004).
4. R. Baier, A.H. Mueller, D. Schiff, D.T. Son, Phys. Lett. B **539**, 46 (2002).
5. P. Arnold, D.T. Son, L.G. Yaffe, Phys. Rev. D **59**, 105020 (1999).
6. St. Mrówczyński, Phys. Rev. C **49**, 2191 (1994).
7. A. Rebhan, P. Romatschke, M. Strickland, Phys. Rev. Lett. **94**, 102303 (2005).
8. P. Arnold, J. Lenaghan, G.D. Moore, L.G. Yaffe, Phys. Rev. Lett. **94**, 072302 (2005).
9. J. Randrup, St. Mrówczyński, Phys. Rev. C **68**, 034909 (2003).
10. P. Romatschke, M. Strickland, Phys. Rev. D **68**, 036004 (2003).
11. P. Arnold, J. Lenaghan, G.D. Moore, JHEP **0308**, 002 (2003).
12. A. Dumitru, Y. Nara, Phys. Lett. B **621**, 89 (2005).
13. N.A. Krall, A.W. Trivelpiece, *Principles of Plasma Physics* (McGraw-Hill, New York, 1973).
14. St. Mrówczyński, Acta Phys. Pol. B **37**, 427 (2006).
15. St. Mrówczyński, Phys. Lett. B **393**, 26 (1997).
16. St. Mrówczyński, M.H. Thoma, Phys. Rev. D **62**, 036011 (2000).
17. P. Arnold, J. Lenaghan, Phys. Rev. D **70**, 114007 (2004).
18. St. Mrówczyński, A. Rebhan, M. Strickland, Phys. Rev. D **70**, 025004 (2004).
19. R.D. Pisarski, arXiv:hep-ph/9710370.
20. P. Arnold, G.D. Moore, L.G. Yaffe, JHEP **0301**, 039 (2003).
21. E. Braaten, R.D. Pisarski, Phys. Rev. D **45**, 1827 (1992).
22. J.C. Taylor, S.M.H. Wong, Nucl. Phys. B **346**, 115 (1990).
23. J.P. Blaizot, E. Iancu, Nucl. Phys. B **417**, 608 (1994).
24. P.F. Kelly, Q. Liu, C. Lucchesi, C. Manuel, Phys. Rev. D **50**, 4209 (1994).
25. H.T. Elze, U.W. Heinz, Phys. Rep. **183**, 81 (1989).
26. St. Mrówczyński, Phys. Rev. D **39**, 1940 (1989).
27. U.W. Heinz, Ann. Phys. (N.Y.) **161**, 48 (1985).
28. J.P. Blaizot, E. Iancu, Phys. Rep. **359**, 355 (2002).
29. P. Arnold, G.D. Moore, L.G. Yaffe, Phys. Rev. D **72**, 054003 (2005).
30. A. Rebhan, P. Romatschke, M. Strickland, JHEP **0509**, 041 (2005).
31. P. Arnold, G.D. Moore, Phys. Rev. D **73**, 025006 (2006).
32. P. Romatschke, A. Rebhan, arXiv:hep-ph/0605064.
33. C. Manuel, St. Mrówczyński, arXiv:hep-ph/0606276.
34. A. Dumitru, Y. Nara, Eur. Phys. J. A **29**, 65 (2006).
35. A. Dumitru, Y. Nara, M. Strickland, arXiv:hep-ph/0604149.
36. P. Romatschke, R. Venugopalan, Phys. Rev. Lett. **96**, 062302 (2006).
37. P. Romatschke, R. Venugopalan, Eur. Phys. J. A **29**, 71 (2006).
38. P. Romatschke, R. Venugopalan, Phys. Rev. D **74**, 045011 (2006).
39. E. Iancu, R. Venugopalan, in *Quark-Gluon Plasma 3*, edited by R.C. Hwa, X.N. Wang (World Scientific, Singapore, 2004).
40. C. Manuel, St. Mrówczyński, Phys. Rev. D **72**, 034005 (2005).
41. M. Asakawa, S.A. Bass, B. Muller, Phys. Rev. Lett. **96**, 252301 (2006).
42. M. Asakawa, S.A. Bass, B. Muller, arXiv:hep-ph/0608270.